DOI: 10.1002/ejic.201100575

A Modular Approach towards the Synthesis of Target-Specific MRI Contrast Agents

Peter Verwilst,[a] Svetlana V. Eliseeva,[a] Sophie Carron,[a] Luce Vander Elst,[b] Carmen Burtea,[b] Geert Dehaen,[a] Sophie Laurent,[b] Koen Binnemans,[a] Robert N. Muller,[b] Tatjana N. Parac-Vogt,[a] and Wim M. De Borggraeve*[a]

Keywords: Imaging agents / Lanthanides / Click chemistry / Macrocyclic ligands / Gadolinium

In this paper, a modular pathway towards the synthesis of new specific MRI contrast agents and their luminescent analogues is described. Using two azide-bearing probes, 3β-deoxycholic acid and *c*RGDfK(N_3), we performed a "click" reaction with an alkyne-bearing 1,4,7,10-tetraazacyclododecane-1,4,7,10-tetraacetic acid (DOTA) analogue, yielding a possible blood-pool contrast agent, as well as a contrast agent with a high affinity for cells expressing $\alpha_v\beta_3$ integrin. The nuclear magnetic relaxation dispersion (NMRD) profiles and human serum albumin (HSA) titration of the contrast agent bearing deoxycholic acid show that this contrast agent interacts with HSA. T_1 measurements of Jurkat T cells in the presence of the contrast agent proved the retention of the integrin-binding property of the RGD-bearing contrast agent.

Introduction

The advances in the field of targeted drug design have prompted the research for equally specific diagnostic tools, since the first step in disease treatment is diagnosis. Among the currently used diagnostic tools, MRI (magnetic resonance imaging) is one of the most powerful and convenient methods to capture a high-resolution image in a noninvasive way. An MR image is a three dimensional mapping of certain NMR parameters, such as the relaxation rate of water protons. While not all MRI examinations require contrast enhancement, Gd^{III}-based contrast agents are frequently used.[1]

In this work we present a modular and convergent approach towards the synthesis of DOTA-type contrast agents decorated with specific ligands, which can be used to obtain a smart image of certain organs or tissues. We used the Cu^{I}-catalyzed reaction between alkynes and azides to form 1,4-disubstituted 1,2,3-triazoles.[2] This so-called "click" reaction was chosen because of the mild reaction conditions and excellent chemoselectivity as well as its high tolerance for various functional groups. This reaction has been used in the synthesis of MRI contrast agents and has thus proved its applicability.[3] In the recent literature, the "click" reaction was mainly used as a tool to augment the intensity of the contrast agent by multimerization of gadolinium-containing probes, rather than improving the selectivity.[3a,3c,3d,3f] The approach described in this work is not limited to the two examples described here and can be used whenever an azide-labeled specific ligand or probe can be synthesized (Figure 1). In view of the popularity of the "click chemistry" concept,[4] many ligands and probes are currently available in their azide form.

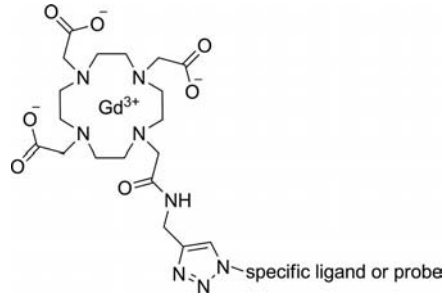

Figure 1. General structure of DOTA-derived specific MRI contrast agents.

As a first example, an RGD-mimetic[5] was used as a high-affinity ligand for the $\alpha_v\beta_3$ integrin. This integrin is expressed on the surface of activated endothelial cells[6] and plays a key role in the formation of atherosclerotic plaques[7] and tumor neovascularization.[8] Binding of the small-molecule MRI agent to the activated tissues causes a local immobilization and concentration of contrast agent and hence achieves a better contrast, which allows the detection of these types of tissues.[9]

[a] Molecular Design and Synthesis, Chemistry Department, Katholieke Universiteit Leuven,
Celestijnenlaan 200F, 3001 Leuven, Belgium
E-mail: Wim.Deborggraeve@chem.kuleuven.be
[b] Laboratoire de RMN et d'Imagerie Moléculaire, Service de Chimie Générale, Organique et Biomédicale, Faculté de Médicine et de Pharmacie, Université de Mons,
7000 Mons, Belgium

Supporting information for this article is available on the WWW under http://dx.doi.org/10.1002/ejic.201100575.

As a second example, an analogue of deoxycholic acid, a naturally occurring bile acid, was used. It has been shown before that conjugates of bile acids with contrast agents give rise to hepatospecific contrast agents[10] with a prolonged lifetime in blood, due to an interaction with human serum albumin (HSA).[11] HSA is the most abundant protein in blood plasma, and this abundance makes it an ideal target for blood-pool contrast agents. The covalent or noncovalent binding of a small-molecule MRI agent to a slow-moving large protein is a well-established method to increase the relaxation rate of protons at a relatively high field[12] and therefore creates a better contrast. HSA-specific contrast agents can thus be used for mapping blood vessels or detecting constrictions.[1d,11,13]

Results and Discussion

Synthesis

3α-Methylsulfonyldeoxycholic acid (**2**) was synthesized from deoxycholic acid (**1**) by using methylsulfonyl chloride in pyridine.[14] Subsequently, nucleophilic displacement of mesylate **2** by sodium azide in DMF yielded the desired 3β-azidodeoxycholic acid (**3**) in good yields (Scheme 1). It proved to be unnecessary to protect the acid functionality in the synthesis of azide **3**, thus the need for a protection and deprotection step was eliminated.[15]

Ligand **L** was prepared according to a literature procedure in three steps from 1,4,7,11-tetraazacyclododecane.[3d,16] Complexation of ligand **L** with Eu^{III} and Gd^{III} was performed by adding a slight excess of $EuCl_3 \cdot 6H_2O$ or $GdCl_3 \cdot 6H_2O$ to an aqueous solution of **L**. The solution was neutralized with KOH and stirred for several hours at 60 °C. Subsequently, free Ln^{III} ions were removed by treatment with CHELEX® beads to yield complexes **ML**. All complexes show a strong IR absorbance around 1600 cm^{-1} characteristic for $\nu_{as}(COO^-)$,[17] which confirms the deprotonation of the ligand and formation of the carboxylate salts (see Supporting Information).

The "click" reaction was performed at 40 °C for 2 hours to yield the desired conjugates **ML-DCA** and **ML-RGD** (Scheme 2).

Photophysical Properties of EuL, EuL-DCA, and EuL-RGD

The luminescence properties of the Eu^{III} complexes were studied. Excitation spectra of aqueous solutions of **EuL**, **EuL-DCA**, and **EuL-RGD** (Figure S1, Supporting Information) present bands mostly due to f–f transitions of the Eu^{III} ion along with a weak broad ligand band below 320 nm. These spectrum profiles reflect a weak sensitization of Eu^{III} emission by organic ligands and are typical for Eu^{III} complexes of DOTA derivatives without extended

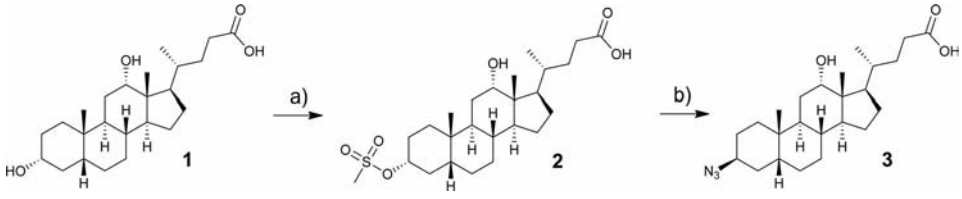

Scheme 1. Synthesis of 3β-azidodeoxycholic acid (**3**) (a) pyridine, methylsulfonyl chloride, 0 °C → room temp., 3 h, 81% (b) NaN_3, DMF, 70 °C, 24 h, 85%.

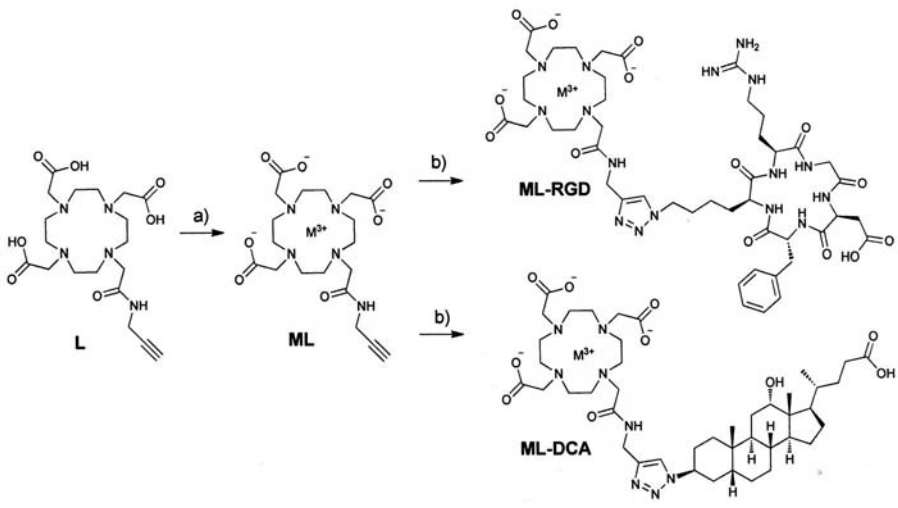

Scheme 2. Synthesis of **ML**, **ML-RGD** and **ML-DCA** (a) $MCl_3 \cdot 6H_2O$, H_2O, 60 °C, overnight, 60–63% (b) corresponding azide, sodium ascorbate, $CuSO_4 \cdot 5H_2O$, H_2O, or H_2O/*t*BuOH, 2 h, 40 °C, 59–68% (M = Eu or Gd).

conjugated substituents.[18] Under UV excitation in the range 280–320 nm, all Eu^{III} complexes display only characteristic red luminescence due to $^5D_0 \rightarrow {}^7F_J$ (J = 0–4) transitions. The crystal-field splittings of the bands undergo very slight variation, while some changes in emission probabilities to different J sublevels are observed. This can be explained by high, variable coordination numbers of lanthanide ions and by the flexibility of cyclen derivatives.[19] It is well-documented that the luminescence properties of lanthanide ions, and especially those of Eu^{III}, are strongly dependent on the nature of the coordination environment and its symmetry.[20] Thus, the relative integrated intensity of the hypersensitive $^5D_0 \rightarrow {}^7F_2$ transition, which is almost equal to that of the magnetic dipole $^5D_0 \rightarrow {}^7F_1$ transition in **EuL**, increases by a factor of about 1.3 to 1.7 when going from **EuL** to **EuL-DCA** and **EuL-RGD**, respectively (Table S1, Supporting Information).

In addition, the highly forbidden $^5D_0 \rightarrow {}^7F_0$ transition has a relatively large intensity in the emission spectra of all of the Eu^{III} complexes, having 11–14% of the intensity of the magnetic dipole $^5D_0 \rightarrow {}^7F_1$ transition (Table S1 and Figure S2, Supporting Information). This is an indication of pseudo-C_4 symmetry around the Eu^{III} ion, which is further reflected in the crystal-field splitting of the f–f transitions (Figure 2).

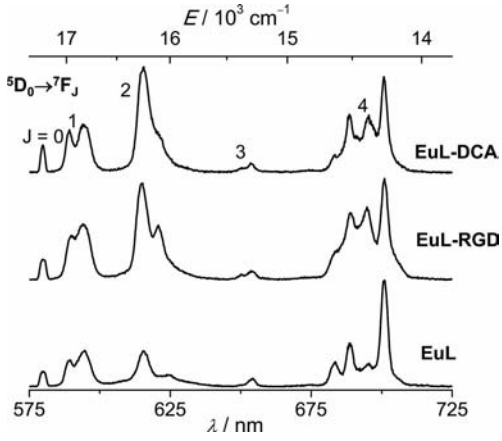

Figure 2. Normalized and corrected emission spectra of Eu^{III} complexes in H_2O (c = 0.5 mM, λ_{ex} = 280–320 nm, room temperature).

Luminescence lifetimes (τ_{obs}) were determined in water (τ_{H2O}) and deuterium oxide (τ_{D2O}) to assess the hydration state of the lanthanide ions and provide additional information on their coordination environment (Table 1). The number of inner-sphere water molecules (q) was calculated from the general relation expressed in Equation (1),[21] where A = 1.2 and B = 0.25 for Eu^{III}, $\Delta k_{obs} = 1/\tau_{H2O} - 1/\tau_{D2O}$ and $q^N = 1$.

$$q(\mathrm{Eu}) = A(\Delta k_{obs} - B - 0.075q^N) \quad (1)$$

Calculated q values for **EuL**, **EuL-DCA**, and **EuL-RGD** range between 1.2–1.3, which are consistent with values for monohydrated complexes.

In order to have a better understanding of the coordination number in vivo, the hydration number of the **EuL-RGD** and **EuL-DCA** complexes were also determined in the presence of HSA (Table 2).

Table 1. Luminescence lifetimes of **EuL**, **EuL-DCA** and **EuL-RGD** (c = 0.5 mM) and calculated hydration numbers.

Compound	Solvent	τ_{obs} (ms)[a]	q[b]
EuL	H_2O	0.58(1)	1.2
	D_2O	2.30(2)	
EuL-RGD	H_2O	0.58(1)	1.2
	D_2O	2.31(2)	
EuL-DCA	H_2O	0.49(1)	1.3
	D_2O	1.60(1)	

[a] Under 320 nm excitation, room temperature, 2σ values between parentheses. [b] Estimated error: 10–20%.

Table 2. Luminescence lifetimes of **EuL-DCA**, and **EuL-RGD** (c = 0.5 mM) in the presence of HSA (c = 0.5 mM) and calculated hydration numbers.

Compound	Solvent	τ_{obs} (ms)[a]	q[b]
EuL-RGD	H_2O	0.56(2)	1.1
	D_2O	1.75(2)	
EuL-DCA	H_2O	0.67(2)	0.6
	D_2O	1.52(2)	

[a] Under 320 nm excitation, room temperature; 2σ values given between parentheses. [b] Estimated error: 10–20%.

Upon addition of HSA, the crystal-field splitting of $^5D_0 \rightarrow {}^7F_J$ (J = 0–4) transitions is almost the same, indicating that the coordination environment around Eu^{III} remains quite similar (Figure S3, Supporting Information). However, the hydration number of **EuL-DCA** is lowered to 0.6 for solutions upon addition of HSA, as a result of (i) partial substitution of inner-sphere water molecules by functional groups of HSA[22] and/or (ii) changes in second-sphere interactions.[23]

^{17}O Relaxometry of GdL-RGD and GdL-DCA

The residence time of the water molecules coordinated to the contrast agent (τ_M) is a key factor of the relaxivity (the relaxivity is defined as the increase in the relaxation rate induced by 1 mmol of paramagnetic center per liter) and can be estimated trough the analysis of the temperature dependence of the transverse relaxation of the ^{17}O resonance of bulk water in solutions of the gadolinium complexes.[13e,24]

The variations with temperature of the bulk water transverse relaxation rate of the ^{17}O resonance in **GdL-RGD** and **GdL-DCA** are quite similar, and the maxima of the reduced transverse paramagnetic relaxation rate are observed at temperatures of 325 to 330 K (Figure 3).

As described previously,[13e,24d,24e,25] the experimental data were fitted to determine the following parameters (Table 3): τ_M, the residence time of the water molecules coordinated to the contrast agent; $\Delta H^{\neq}$ and $\Delta S^{\neq}$, the enthalpy and entropy of activation, respectively, of the water exchange process; $A/\hbar$, the hyperfine coupling constant between the oxygen nucleus of the bound water molecule and the Gd^{III} ion; B, a parameter related to the mean square of

Table 3. Parameters obtained by the theoretical adjustment of the ^{17}O experimental NMR spectroscopic data. The top entries relate to the first fitting, the bottom entries relate to the fitting in which E_V was set to 1 kJ mol^{-1}.

Compound	τ_M^{310} (ns)	$\Delta H^{\neq}$ (kJ mol^{-1})	$\Delta S^{\neq}$ (J mol^{-1} K^{-1})	$A/\hbar$ (10^6 rad s^{-1})
GdL-RGD	352 ± 26	53.30 ± 0.13	50.5 ± 0.2	–3.9 ± 0.2
	343 ± 10	53.30 ± 0.07	50.6 ± 0.2	–3.7 ± 0.4
GdL-DCA	435 ± 28	45.90 ± 0.08	24.6 ± 0.3	–3.5 ± 0.3
	439 ± 63	45.80 ± 0.02	24.4 ± 0.5	–3.5 ± 0.4
Compound	B (10^{20} s^{-2})	τ_V^{298} (ps)	E_V (kJ mol^{-1})	q[a]
GdL-RGD	5.0 ± 0.6	13.10 ± 1.65	5.16 ± 2.38	1
	4.9 ± 0.2	12.80 ± 0.48	1.0[a]	1
GdL-DCA	10.2 ± 0.8	22.7 ± 1.8	0.11 ± 19.20	1
	8.9 ± 1.6	20.0 ± 3.5	1.0[a]	1

[a] Fixed parameter.

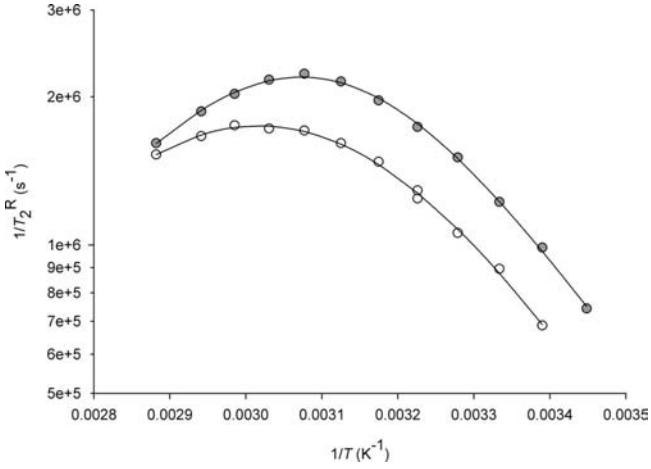

Figure 3. Temperature dependence of the reduced transverse relaxation rate of ^{17}O at 11.75 T of **GdL-DCA** (open circles, 5.8 mM) and **GdL-RGD** (gray circles, 12.7 mM).

the zero-field-splitting energy Δ^2 ($B = 2.4\Delta^2$); τ_V, the correlation time modulating the electronic relaxation of Gd^{III}, and E_V, the activation energy related to τ_V. The value of q was fixed to 1.

It is to be noted that in a first fitting, the error on the E_V value of **GdL-DCA** was very large (Table 3). New fittings were then performed with a value of E_V fixed to 1 kJ mol^{-1}.[26] The τ_M values obtained with both types of fittings are very similar. However, the parameters related to the electronic relaxation have to be considered with caution, since no data point was obtained in the fast exchange regime.

Proton NMRD of GdL-RGD and GdL-DCA

The proton nuclear magnetic relaxation dispersion (NMRD) profile of longitudinal relaxivity in water of **GdL-RGD** was measured at 310 K at a 2.12 mM concentration (Figure 4); the profile is typical for a low-molecular-weight Gd complex. The proton NMRD profile of **GdL-DCA** in water at 310 K at a concentration of 0.97 mM revealed a very high relaxivity at all magnetic fields, and there was a slight hump around 20–60 MHz (Figure S4, Supporting Information). This hump can be explained by self-aggregation of the contrast agent. To determine the concentration at which self-aggregation occurs, the paramagnetic relaxation rate was measured at 20 MHz and 310 K, with increasing concentrations of **GdL-DCA**, showing a normal linear dependence of the relaxation rate on the concentration up to 0.30 mM; above this concentration a deviation from the linear dependence, caused by self-aggregation, was observed (Figure S5, Supporting Information).

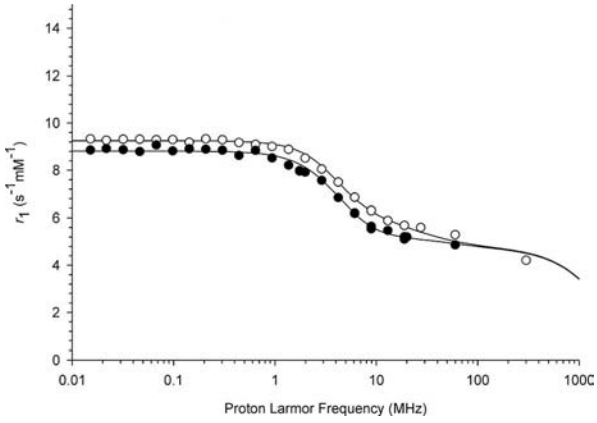

Figure 4. NMRD relaxivity profiles of **GdL-RGD** (open circles) and **GdL-DCA** (black dots) at 310 K, the lines correspond to the theoretical fittings of the data points.

The proton NMRD profile of **GdL-DCA** at 310 K was repeated at a concentration of 0.29 mM, revealing a profile very similar to that of **GdL-RGD** (Figure 4).

The theoretical adjustment of the NMRD profiles takes into account the inner-sphere[27] and the outer-sphere[28] contributions to the paramagnetic relaxation rate. Some parameters were fixed during the fitting procedure: q, the hydration number ($q = 1$); d, the distance of closest approach ($d = 0.36$ nm); D, the relative diffusion constant ($D = 3.3 \times 10^{-9}$ m^2 s^{-1}),[29] and r, the distance between the Gd^{III} ion and the proton nuclei of water ($r = 0.31$ nm). The value of τ_M was also set to that determined by ^{17}O relaxometry. The results of this fitting can be found in Table 4, where they are compared to those for GdDOTA (Dotarem®),

where τ_R is the rotational correlation lifetime, τ_{SO} is the electronic relaxation rate at zero field, and τ_V is the correlation time modulating the electronic relaxation of Gd^{III}.

Table 4. Values of τ_R, τ_{SO}, and τ_V obtained from the proton NMRD profiles, compared to those for GdDOTA.

Compound	r_1 (s^{-1} mM^{-1})[a]	τ_R^{310} (ps)	τ_{SO}^{310} (ps)	τ_V^{310} (ps)
GdDOTA[b]	3.5	53 ± 1	404 ± 24	7 ± 1
GdL-RGD	5.7	112 ± 4	122 ± 4	16 ± 1
GdL-DCA	5.6	120 ± 3	128 ± 3	28 ± 3

[a] At 20 MHz and 310 K. [b] From ref.[25]

As expected, the theoretical adjustments of ^{17}O relaxometry reveal an increased value of τ_M as a result of the amide bond near the Gd^{III} ion. The fitted τ_R value is in agreement with the expected value considering the size of the complexes. The agreement between the fitted parameters characterizing the electronic relaxation rates obtained either from the ^{17}O data (B and τ_V) or from the proton NMRD data [τ_{SO} and τ_V, with $\tau_{SO} = (5B\tau_V)^{-1}$] is poor. The differences between the values obtained by each experimental approach can be related, firstly, to the fact that the influence of the electronic relaxation times is predominant at low fields in the proton NMRD curves of small complexes whereas the ^{17}O data are obtained at much higher field and, secondly, to the simplified model used for the analysis of our ^{17}O T_2 data.

HSA Binding of GdL-RGD and GdL-DCA

The binding of **GdL-RGD** and **GdL-DCA** with HSA was assessed by performing a titration, in which the concentration of HSA was kept constant at 4% and the concentration of the complex was varied.

As expected, **GdL-RGD** showed no significant binding with HSA (Figure 5), which allows the molecule to bind to its target without interference from HSA.

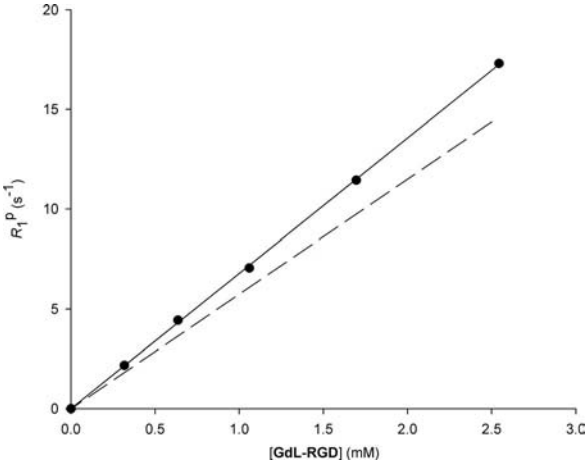

Figure 5. Titration of HSA with **GdL-RGD** at 20 MHz and 310 K, in water (dotted line) and in the presence of 4% HSA (black dots and solid line).

In the case of **GdL-DCA**, a strong binding of the contrast agent to HSA was observed (Figure 6).

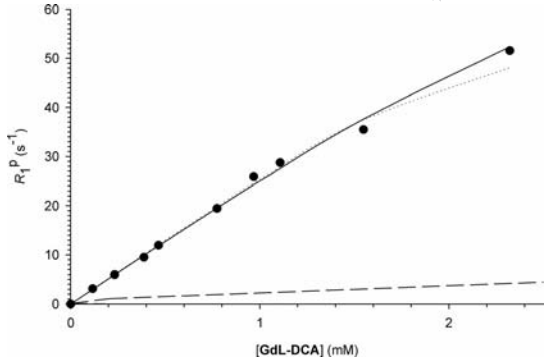

Figure 6. Titration of HSA with **GdL-DCA** at 20 MHz and 310 K, in the presence of 4% HSA [black dots, solid line (N = 4) and dotted line (N = 3)] extrapolated linear behavior in water (dashed line).

This was further confirmed by the proton NMRD profile of a 0.97 mM concentration of **GdL-DCA** in the presence of 4% HSA. The profile shows an elevated value of the relaxivity and a hump around 20–60 MHz, caused by binding of the contrast agent with HSA (Figure 7).

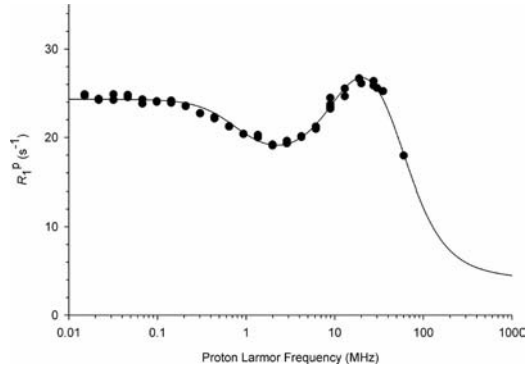

Figure 7. NMRD profile of **GdL-DCA** (0.97 mM) in the presence of 4% HSA at 310 K. The line through the data is drawn to guide the eyes.

The data of the titration experiment could be fitted by using Equation (2), where p^0 and s^0 are the concentrations of protein and contrast agent, respectively, r_1^c and r_1^f are the relaxivity of the bound and free complexes, respectively, N is the number of independent and equivalent binding sites, and K is their association constant (Table 5). The best fit was obtained with N = 4 (Figure 6).

$$R_1^p = 1000 \times \left(\left[r_1^f \times s^0 \right] + \frac{1}{2}\left[r_1^c - r_1^f \right] \times \left[\left\{ N \times p^0 \right\} + s^0 + K^{-1} - \sqrt{\left\{ \left(N \times p^0 \right) + s^0 + K^{-1} \right\}^2 - 4 \times N \times s^0 \times p^0} \right] \right) \quad (2)$$

Table 5. Fitted parameters of the titration experiment to determine the binding constant of **GdL-DCA** to HSA.

r_1^f (s^{-1} mM^{-1})	r_1^c (s^{-1} mM^{-1})	N	K (M^{-1})
5.6	27	4	6760 ± 3270

These data suggest that in the concentration range extending from 0.1 mM to 1 mM, more than 90% of **GdL-DCA**

is bound to HSA. An ultrafiltration experiment performed on a sample containing **GdL-DCA** (0.52 mM) and HSA (4%) confirmed these results (94% of the **GdL-DCA** is bound to HSA, Figure S6, Supporting Information). The binding of **GdL-DCA** to HSA is thus better than that for MS-325[13e] and similar to the binding of B22956/1, a Gd-DTPA derivative substituted by deoxycholic acid.[11]

In Vitro Validation of the Interaction of GdL-RGD with $\alpha_v\beta_3$ Integrin by Proton Relaxometry

GdL-RGD was evaluated on Jurkat T cells to confirm the preservation of its affinity for integrins. The proton longitudinal time, T_1, was determined for a sample containing stimulated Jurkat T cells, which overexpress α_v integrins, and **GdL-RGD**, as well as for a series of control samples (Table 6).

Table 6. Proton relaxometric data at 60 MHz.

Compound	Cells	T_1 (ms)	R_1 (s^{-1})	R_1^{Norm} (s^{-1})
None	Stimulated	2890	0.34608	/
GdL-RGD	Stimulated	2650	0.37736	0.0313
GdDOTA	Stimulated	2860	0.34965	0.0036
None	Nonstimulated	2990	0.33445	/
GdL-RGD	Nonstimulated	2990	0.33445	0
GdDOTA	Nonstimulated	2960	0.33784	0.0034

R_1^{Norm}, the difference between the relaxivity in the presence and absence of a contrast agent, was determined. A 9% relative increase in relaxivity was observed for samples containing stimulated Jurkat T cells and **GdL-RGD**, whereas there was only 1% increase when GdDOTA was used, which confirms the interaction of **GdL-RGD** with the integrins of stimulated Jurkat T cells (Figure 8).

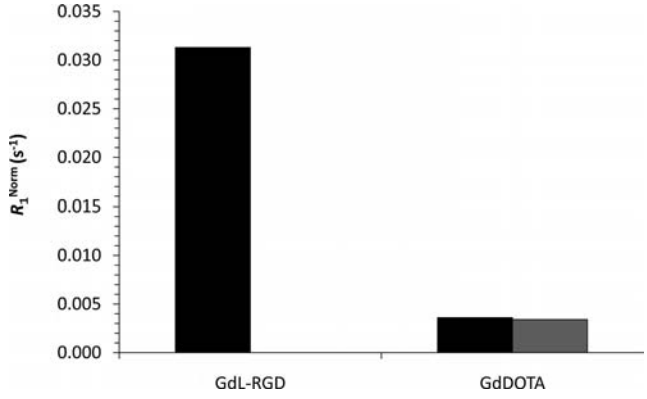

Figure 8. R_1^{Norm} of stimulated cells (black) and nonstimulated cells (gray) at 60 MHz.

Conclusions

Two new contrast agents and their luminescent analogues have been synthesized and characterized. For the contrast agent bearing deoxycholic acid (**GdL-DCA**), HSA titrations proved its interaction with HSA, and the NMRD profile in the presence of HSA further reflected this, by showing an increased relaxivity and the presence of a hump in the profile, due to aggregation with HSA. For the contrast agent bearing cyclic RGD peptide (**GdL-RGD**), an increased relaxivity was observed in T_1 measurements only in the presence of integrin-expressing Jurkat T cells, proving the retention of integrin-binding ability by this contrast agent.

The modular synthetic pathway described can be further implemented in the synthesis of new specific MRI contrast agents.

Experimental Section

All chemicals were purchased from Acros (Belgium), Sigma-Aldrich (Belgium), or ABCR (Germany) and were used without further purification. The *c*RGDfK(N_3)[5d] was purchased from SBS Genentech (Beijing, China). All ^1H and ^{13}C NMR spectra were recorded with a Bruker Avance 400 or 600 spectrometer. The LC/MS data were collected by using an Agilent 1100 system coupled to an Agilent 6110 single-quadrupole MS system. A Grace Prevail RP-C_{18} column (150 mm × 2.1 mm, particle size 3 μm) was employed. Preparative HPLC was performed by using a Waters Delta 600 system equipped with a Waters 996 Photo Diode Array detector. A Phenomenex Luna C_{18} column (150 mm × 21.20 mm, particle size 5 μm) was employed. All infrared spectra were recorded with a Bruker Alpha-P IR apparatus, and the data was processed with OPUS 6.5 software. Melting points were determined by using a Reichert-Jung Thermovar apparatus.

Syntheses

Mesylate 2: A solution of deoxycholic acid (**1**) (98 mg, 0.25 mmol) in pyridine (5 mL) was stirred at 0 °C. Methylsulfonyl chloride (23 μL 0.30 mmol) was added dropwise, and the solution was stirred at 0 °C for 30 min. The reaction mixture was warmed to room temperature and was stirred for an additional 3 h. To this reaction mixture was added HCl (100 mL, 2 N), and the solution was extracted with EtOAc (3 × 100 mL). The solvent was removed in vacuo, and chromatographic separation (silica gel, EtOAc) yielded mesylate **2**. Yield: 95 mg, 81%. M.p.: 168 °C. ^1H NMR (400 MHz, [D_6]DMSO): δ = 11.89 (br. s, 1 H, COOH), 4.56 (m, 1 H, 3-H), 4.17 (br. s, 1 H, 12-OH), 3.78 (s, 1 H, 12-H), 3.14 (s, 3 H, CH_3SO_3), 2.23 (m, 1 H, 22-H), 2.10 (m, 1 H, 22-H), 1.92–0.95 (m, 24 H), 0.91 (d, J = 6 Hz, 3 H, 21-H_3), 0.87 (s, 3 H, 19-H_3), 0.60 (s, 3 H, 18-H_3) ppm. ^{13}C NMR (100 MHz, [D_6]DMSO): δ = 175.37 (C-24), 82.62 (C-3), 71.51 (C-12), 47.84 (C-14), 46.67 (C-17), 46.48 (C-13), 41.77 (C-5), 38.35 (C-sulfonate), 35.94 (C-8), 35.39 (C-9), 34.82 (CH_2), 33.95 (C-10), 33.26 (CH_2), 33.18 (C-20), 31.28 (C-22), 31.21 (CH_2), 28.92 (CH_2), 27.71 (CH_2), 27.59 (CH_2), 26.94 (CH_2), 26.26 (CH_2), 23.90 (CH_2), 23.06 (C-19), 17.39 (C-21), 12.87 (C-18) ppm. IR (neat): $\tilde{\nu}$ = 3536, 3392, 2931, 2868, 1734, 1706 cm^{-1}. ESI-MS ($C_{25}H_{42}O_6S$): m/z = 471 $[M + H]^+$, 493 $[M + Na]^+$, 963 $[2M + Na]^+$.

Azide 3: NaN_3 (20 mg, 0.31 mmol) was added to a solution of mesylate **2** (47 mg, 0.10 mmol) in DMF (5 mL), and the suspension was stirred at 70 °C for 24 h. HCl (100 mL, 2 N) was added to this reaction mixture, and the solution was extracted with EtOAc (3 × 100 mL). The solvent was removed in vacuo, and chromatographic separation (silica gel, EtOAc) yielded azide **3**. Yield: 35 mg, 85%. M.p.: 78 °C. ^1H NMR (600 MHz, [D_6]DMSO): δ = 11.93 (br. s, 1 H, COOH), 4.17 (br. s, 1 H, 12-OH), 4.07 (s, 1 H, 3-H), 3.79 (s, 1 H, 12-H), 2.22 (m, 1 H, 22-H), 2.10 (m, 1 H, 22-H), 2.05–0.96 (m, 24 H), 0.91 (m, 3 H, 21-H_3), 0.88 (s, 3 H, 19-H_3), 0.61 (s, 3 H,

18-H_3) ppm. ^{13}C NMR (150 MHz, [D_6]DMSO): δ = 175.41 (C-24), 71.54 (C-12), 58.74 (C-3), 47.92 (C-14), 46.68 (C-17), 46.51 (C-13), 37.58 (C-5), 35.87 (C-8), 35.41 (C-9), 34.61 (C-10), 32.84 (C-20), 31.28 (C-22), 31.35 (CH_2), 30.94 (CH_2), 30.11 (CH_2), 29.15 (CH_2), 27.60 (CH_2), 26.62 (CH_2), 26.25 (CH_2), 24.51 (CH_2), 23.90 (CH_2), 23.87 (C-21), 17.40 (C-19), 12.90 (C-18) ppm. IR (neat): $\tilde{\nu}$ = 3514, 2929, 2089, 1713, 1650 cm^{-1}. ESI-MS ($C_{24}H_{39}N_3O_3$): *m*/*z* = 418 [M + H]$^+$, 440 [M + Na]$^+$, 857 [2M + Na]$^+$.

General Procedure for the Synthesis of ML: L (60 mg, 0.136 mmol) was dissolved in deionized water (5 mL), $LnCl_3 \cdot 6H_2O$ (0.15 mmol) was added, and the pH was adjusted to 6 with a solution of KOH (0.1 M). The solution was stirred overnight at 60 °C. Subsequently, the solution was treated with CHELEX-100® (twice), and the solvent was removed in vacuo. The completeness of free lanthanide removal was checked by using the test with an Arsenazo III indicator.[30] When necessary, a third treatment with CHELEX-100® was performed. Chromatographic purification (HPLC, Solvent A: H_2O + 0.1% HCOOH, Solvent B: MeOH, 0% B → 100% B, 30 min) yielded the corresponding Ln^{III} complexes.

Europium Complex EuL: Yield: 51 mg, 63%. HPLC: t_r = 8.79 min. Purity (215 nm): 96.05%. ESI-MS ($C_{19}H_{28}EuN_5O_7$): *m*/*z* = 1179 [2M + H]$^+$, 885 [3M + 2 H]$^{2+}$, 590 [M + H]$^+$, 394 [2M + 3 H]$^{3+}$, 295 [M + 2 H]$^{2+}$. IR (neat): $\tilde{\nu}$ = 3396, 3253, 3077, 2858, 1601 cm^{-1}.

Gadolinium Complex GdL: Yield: 49 mg, 60%. HPLC: t_r = 7.67 min. Purity (215 nm): 88.07%. ESI-MS ($C_{19}H_{28}GdN_5O_7$): *m*/*z* = 1193 [2M + H]$^+$, 894 [3M + 2 H]$^{2+}$, 597 [M + H]$^+$, 399 [2M + 3 H]$^{3+}$, 298 [M + 2 H]$^{2+}$. IR (neat): $\tilde{\nu}$ = 3399, 3233, 3075, 2987, 2860, 1604 cm^{-1}.

General Procedure for the "Click" Reactions: ML (34 μmol) and the corresponding azide (37 μmol) were dissolved in deionized water (1 mL) or *t*BuOH/H_2O (1:1) (1 mL). $CuSO_4 \cdot 5H_2O$ (3.4 μmol; 0.1 mL of a 34 mM solution) and sodium ascorbate (17 μmol; 0.1 mL of a 170 mM solution) were added, and the solution was stirred for 2 h at 40 °C under an Ar atmosphere. The solvent was removed in vacuo, and chromatographic purification (HPLC) yielded the corresponding "clicked" Ln^{III} complexes.

Europium Complex EuL-RGD: Yield: 25 mg, 59%. HPLC (Solvent A: H_2O + 0.1% HCOOH, Solvent B: ACN, 10% B → 35% B, 40 min): t_r = 11.56 min. Purity (215 nm): 98.44%. ESI-MS ($C_{47}H_{69}EuN_{16}O_{14}$): *m*/*z* = 1222 [M + H]$^+$, 814 [2M + 3 H]$^{3+}$, 611 [M + 2 H]$^{2+}$, 408 [M + 3 H]$^{3+}$. IR (neat): $\tilde{\nu}$ = 3264, 3062, 2941, 2867, 1601 cm^{-1}.

Gadolinium Complex GdL-RGD: Yield: 29 mg, 68%. HPLC (Solvent A: H_2O + 0.1% HCOOH, Solvent B: ACN, 10% B → 35% B, 40 min): t_r = 11.44 min. Purity (215 nm): 96.88%. ESI-MS ($C_{47}H_{69}GdN_{16}O_{14}$): *m*/*z* = 1225 [M + H]$^+$, 818 [2M + 3 H]$^{3+}$, 614 [M + 2 H]$^{2+}$, 409 [M + 3 H]$^{3+}$. IR (neat): $\tilde{\nu}$ = 3272, 3062, 2942, 2859, 1615 cm^{-1}.

Europium Complex EuL-DCA: Yield: 21 mg, 61%. HPLC (Solvent A: H_2O + 0.1% HCOOH, Solvent B: ACN, 20% B → 80% B, 20 min): t_r = 14.65 min. Purity (215 nm): 98.50%. ESI-MS ($C_{43}H_{67}EuN_8O_{10}$): *m*/*z* = 1345 [4M + 3 H]$^{3+}$, 1008 [M + H]$^+$, 665 [2M + 3 H]$^{3+}$, 504 [M + 2 H]$^{2+}$. IR (neat): $\tilde{\nu}$ = 3391, 3249, 3078, 2930, 2861, 1602 cm^{-1}.

Gadolinium Complex GdL-DCA: Yield: 22 mg, 65%. HPLC (Solvent A: H_2O + 0.1% HCOOH, Solvent B: ACN, 20% B → 80% B, 20 min): t_r = 14.47 min. Purity (215 nm): 98.55%. ESI-MS ($C_{43}H_{67}GdN_8O_{10}$): *m*/*z* = 1351 [4M + 3 H]$^{+3}$, 1013 [M + H]$^+$, 677 [2M + 3 H]$^{3+}$, 507 [M + 2 H]$^{2+}$. IR (neat): $\tilde{\nu}$ = 3390, 3237, 3078, 2930, 2859, 1602 cm^{-1}.

Spectroscopic Measurements: Photophysical data (excitation, emission spectra, and lifetimes) were recorded with an Edinburgh Instruments FS920 steady state spectrofluorimeter by using freshly prepared aqueous solutions placed into quartz Suprasil® cells (optical path length 1 cm). This instrument is equipped with a 450 W xenon arc lamp, a high energy microsecond flash lamp μF900H, and an extended red-sensitive photomultiplier (185–1010 nm, Hamamatsu R 2658P). All spectra are corrected for the instrumental functions. Luminescence lifetimes under ligand excitation for Eu^{III} complexes were measured by monitoring the $^5D_0 \rightarrow {}^7F_2$ transition at 614 nm. They are the average of at least three independent measurements.

^{17}O Measurements: ^{17}O NMR measurements of solutions were performed at 7.05 T on 2 mL samples contained in 10 mm o.d. tubes with a Bruker AMX-300 spectrometer. The temperature was regulated by air or nitrogen flow controlled by a Bruker BVT 2000 unit. ^{17}O transverse relaxation times of distilled water (pH 6.5–7) were measured by using a CPMG sequence and a subsequent two-parameter fit of the data points. The 90° and 180° pulse lengths were 25 and 50 μs, respectively. The ^{17}O T_2 of water in complex solution was obtained from linewidth measurements. All spectra were proton decoupled. The concentration of the samples was lower than 25 mM. The data are presented as the reduced transverse relaxation rate $\{1/T_2^R = 55.55/([\text{Gd complex}] \cdot q \cdot T_2^P)$, where: [Gd complex] is the molar concentration of the complex, *q* is the number of coordinated water molecules, and T_2^P is the paramagnetic transverse relaxation rate$\}$.

Proton NMRD: Proton nuclear magnetic relaxation dispersion (NMRD) profiles were measured with a Stelar Spinmaster FFC fast field cycling NMR relaxometer over a magnetic field strength range extending from 0.24 mT to 0.24 T or with a field cycling relaxometer over a magnetic field range between 0.24 mT and 1.0 T. Measurements were performed on 0.6 mL samples contained in 10 mm o.d. Pyrex tubes. Additional relaxation rates at 20 and 60 MHz were obtained with a Minispec PC-120 and a Minispec mq60 instrument, respectively.

Interaction with HSA: The binding constant and relaxivity of Gd complexes in a 4% solution of HSA were determined by measuring the proton longitudinal relaxation rate at 20 MHz and 310 K as a function of the concentration of the Gd complex.

Ultrafiltration Experiment with HSA: The unbound ligand fraction was separated by using an Amicon Ultra centrifugal filter and Ultracell-10K tube (Millipore) by centrifugation. The free ligand concentration was obtained by proton relaxometry (three to five T_1 measurements). The bound ligand concentration was calculated by subtracting the free ligand concentration from the initial concentration measured by relaxometry. The relative error on the T_1 measurements was 3%.

Culture and Stimulation of Jurkat T Lymphocytes: Jurkat cells (gift from Prof. Oberdan Leo, Free University of Brussels, IBMM, Gosselies, Belgium) were cultured at a concentration of 1×10^6 mL^{-1} in RPMI 1640 medium supplemented with 10% NCS (Newborn Calf Serum) and 1% antibiotic–antimicotic. Jurkat cells were stimulated ($< 10^6$ cells/mL, 37 °C, 48 h) with 1 mg/mL PHA (Phytohemagglutinin) and 30 nM PMA (phorbol-12-myristate-13-acetate) to overexpress α_v integrins.[31]

In Vitro Validation of Integrin Binding: For binding experiments, 5×10^6 cells in 4 mL were incubated (2 h, room temperature, mechanical agitation) with **Gd-RGD** or Gd-DOTA at a concentration of 700 μM. For relaxometric analyses, the final pellet obtained after centrifugation (15 min at 4500 rpm) was resuspended (5×10^6 cells/

sample) in 2% gelatin (0.05 mL) prepared in phosphate-buffered saline (PBS) (150 mM NaCl, 3.2 mM KCl, 6.4 mM $Na_2HPO_4 \cdot 12H_2O$, 1.5 mM KH_2PO_4, pH 7.4) and transferred into minispec tubes. Two samples were prepared for each group, but the samples were then put together (10^7 cells/0.1 mL gelatin) to obtain a strong enough signal. The T_1 measurements were performed with a Bruker Minispec mq60 (at 60 MHz) instrument at 37 °C.

Supporting Information (see footnote on the first page of this article): NMR and IR spectra of **2** and **3**, HPLC analyses and IR spectra of **ML**, **ML-RGD**, and **ML-DCA**, supplementary spectroscopic information of **EuL**, **EuL-RGD**, and **EuL-DCA**, as well as self-aggregation and ultrafiltration experiments of **GdL-DCA**.

Acknowledgments

The authors thank the FWO-Flanders (Fonds Wetenschappelijk Onderzoek - Vlaanderen, project G.0412.09) for financial support and for a visiting postdoctoral fellowship for S. V. E. (project G.0412.09). P. V., S. C. and G. D. would like to thank IWT (Agentschap voor Innovatie door Wetenschap en Technologie) for financial support.

[1] a) P. Caravan, J. J. Ellison, T. J. McMurry, R. B. Lauffer, *Chem. Rev.* **1999**, *99*, 2293–2352; b) E. Terreno, W. Dastrù, D. Delli Castelli, E. Gianolio, S. Geninatti Crich, D. Longo, S. Aime, *Curr. Med. Chem.* **2010**, *17*, 3684–3700; c) A. J. L. Villaraza, A. Bumb, M. W. Brechbiel, *Chem. Rev.* **2010**, *110*, 2921–2959; d) E. Terreno, D. D. Castelli, A. Viale, S. Aime, *Chem. Rev.* **2010**, *110*, 3019–3042.

[2] a) V. V. Rostovtsev, L. G. Green, V. V. Fokin, K. B. Sharpless, *Angew. Chem.* **2002**, *114*, 2708; *Angew. Chem. Int. Ed.* **2002**, *41*, 2596–2599; b) C. W. Tornoe, C. Christensen, M. Meldal, *J. Org. Chem.* **2002**, *67*, 3057–3064.

[3] a) D. J. Mastarone, V. S. R. Harrison, A. L. Eckermann, G. Parigi, C. Luchinat, T. J. Meade, *J. Am. Chem. Soc.* **2011**, *133*, 5329–5337; b) T. L. Mindt, C. Muller, F. Stuker, J.-F. Salazar, A. Hohn, T. Mueggler, M. Rudin, R. Schibli, *Bioconjugate Chem.* **2009**, *20*, 1940–1949; c) J. M. Bryson, W.-J. Chu, J.-H. Lee, T. M. Reineke, *Bioconjugate Chem.* **2008**, *19*, 1505–1509; d) Y. Song, E. K. Kohlmeir, T. J. Meade, *J. Am. Chem. Soc.* **2008**, *130*, 6662–6663; e) G. J. Stasiuk, M. P. Lowe, *Dalton Trans.* **2009**, 9725–9727; f) M. Jauregui, W. S. Perry, C. Allain, L. R. Vidler, M. C. Willis, A. M. Kenwright, J. S. Snaith, G. J. Stasiuk, M. P. Lowe, S. Faulkner, *Dalton Trans.* **2009**, 6283–6285.

[4] H. C. Kolb, M. G. Finn, K. B. Sharpless, *Angew. Chem.* **2001**, *113*, 2056; *Angew. Chem. Int. Ed.* **2001**, *40*, 2004–2021.

[5] a) L. M. De Leon-Rodriguez, Z. Kovacs, *Bioconjugate Chem.* **2008**, *19*, 391–402; b) R. Haubner, H. J. Wester, U. Reuning, R. Senekowitsch-Schmidtke, B. Diefenbach, H. Kessler, G. Stocklin, M. Schwaiger, *J. Nucl. Med.* **1999**, *40*, 1061–1071; c) R. Haubner, H. J. Wester, F. Burkhart, R. Senekowitsch-Schmidtke, W. Weber, S. L. Goodman, H. Kessler, M. Schwaiger, *J. Nucl. Med.* **2001**, *42*, 326–336; d) I. Dijkgraaf, A. Y. Rijnders, A. Soede, A. C. Dechesne, G. W. van Esse, A. J. Brouwer, F. H. M. Corstens, O. C. Boerman, D. T. S. Rijkers, R. M. J. Liskamp, *Org. Biomol. Chem.* **2007**, *5*, 935–944.

[6] W. Cai, G. Niu, X. Chen, *Curr. Pharm. Des.* **2008**, *14*, 2943–2973.

[7] M. Hoshiga, C. E. Alpers, L. L. Smith, C. M. Giachelli, S. M. Schwartz, *Circ. Res.* **1995**, *77*, 1129–1135.

[8] P. C. Brooks, R. A. Clark, D. A. Cheresh, *Science* **1994**, *264*, 569–571.

[9] a) E. Garanger, D. Boturyn, P. Dumy, *Anti-Cancer Agents Med. Chem.* **2007**, *7*, 552–558; b) M. Neeman, A. A. Gilad, H. Dafni, B. Cohen, *J. Magn. Reson. Imag.* **2007**, *25*, 1–12; c) C. Burtea, S. Laurent, O. Murariu, D. Rattat, G. Toubeau, A. Verbruggen, D. Vansthertem, L. V. Elst, R. N. Muller, *Cardiovasc. Res.* **2008**, *78*, 148–157; d) J. A. Park, J. J. Lee, J. C. Jung, D. Y. Yu, C. Oh, S. Ha, T. J. Kim, Y. M. Chang, *ChemBioChem* **2008**, *9*, 2811–2813.

[10] P. L. Anelli, L. Lattuada, V. Lorusso, G. Lux, A. Morisetti, P. Morosini, M. Serleti, F. Uggeri, *J. Med. Chem.* **2004**, *47*, 3629–3641.

[11] a) C. de Haen, P. L. Anelli, V. Lorusso, A. Morisetti, F. Maggioni, J. Zheng, F. Uggeri, F. M. Cavagna, *Invest. Radiol.* **2006**, *41*, 279–291; b) P. L. Anelli, M. Brocchetta, C. De Haen, O. Gazzotti, L. Lattuada, G. Lux, G. Manfredi, P. Morosini, D. Palano, M. Serleti, F. Uggeri, M. Visigalli (Bracco Imaging S. p. A.), U. S. 6461588, **2002**; c) A. La Noce, S. Stoelben, K. Scheffler, J. Hennig, H. M. Lenz, R. La Ferla, V. Lorusso, F. Maggioni, F. Cavagna, *Acad. Radiol.* **2002**, *9 Suppl 2*, S404–406; d) F. M. Cavagna, V. Lorusso, P. L. Anelli, F. Maggioni, C. de Haen, *Acad. Radiol.* **2002**, *9 Suppl 2*, S491–494.

[12] R. B. Lauffer, *Chem. Rev.* **1987**, *87*, 901–927.

[13] a) S. Aime, M. Chiaussa, G. Digilio, E. Gianolio, E. Terreno, *J. Biol. Inorg. Chem.* **1999**, *4*, 766–774; b) F. G. Blankenberg, C. Mari, H. W. Strauss, *Am. J. Cardiovasc. Drugs* **2002**, *2*, 357–365; c) P. Caravan, N. J. Cloutier, M. T. Greenfield, S. A. McDermid, S. U. Dunham, J. W. M. Bulte, J. C. Amedio, R. J. Looby, R. M. Supkowski, W. D. Horrocks, T. J. McMurry, R. B. Lauffer, *J. Am. Chem. Soc.* **2002**, *124*, 3152–3162; d) R. B. Lauffer, D. J. Parmelee, S. U. Dunham, H. S. Ouellet, R. P. Dolan, S. Witte, T. J. McMurry, R. C. Walovitch, *Radiology* **1998**, *207*, 529–538; e) R. N. Muller, B. Raduchel, S. Laurent, J. Platzek, C. Pierart, P. Mareski, L. Vander Elst, *Eur. J. Inorg. Chem.* **1999**, 1949–1955; f) T. N. Parac-Vogt, K. Kimpe, S. Laurent, L. Vander Elst, C. Burtea, F. Chen, R. N. Muller, Y. C. Ni, A. Verbruggen, K. Binnemans, *Chem. Eur. J.* **2005**, *11*, 3077–3086.

[14] G. Wess, W. Kramer, W. Bartmann, A. Enhsen, H. Glombik, S. Mullner, K. Bock, A. Dries, H. Kleine, W. Schmitt, *Tetrahedron Lett.* **1992**, *33*, 195–198.

[15] R. Sharma, F. Majer, V. K. Peta, J. Wang, R. Keaveney, D. Kelleher, A. D. Long, J. F. Gilmer, *Bioorg. Med. Chem.* **2010**, *18*, 6886–6895.

[16] a) J. D. E. Prasuhn, R. M. Yeh, A. Obenaus, M. Manchester, M. G. Finn, *Chem. Commun.* **2007**, 1269–1271; b) R. F. H. Viguier, A. N. Hulme, *J. Am. Chem. Soc.* **2006**, *128*, 11370–11371; c) K. Machitani, H. Sakamoto, Y. Nakahara, K. Kimura, *Anal. Sci.* **2008**, *24*, 463–469.

[17] K. Nakamoto in *Infrared and Raman Spectra of Inorganic and Coordination Compounds*, Wiley-VCH, Weinheim, **2008**, pp. 1–273.

[18] a) J. G. Kang, M. K. Na, S. K. Yoon, Y. Sohn, Y. D. Kim, I. H. Suh, *Inorg. Chim. Acta* **2000**, *310*, 56; b) J. I. Bruce, M. P. Lowe, D. Parker in *The Chemistry of Contrast Agents in Medical Magnetic Resonance Imaging* (Eds.: A. E. Merbach, É. Toth), Wiley-VCH, Weinheim, **2001**, pp. 437–460; c) C. C. Bryden, C. N. Reilley, *Anal. Chem.* **1982**, *54*, 610–615.

[19] R. Delgado, V. Felix, L. M. P. Lima, D. W. Price, *Dalton Trans.* **2007**, 2734–2745.

[20] J.-C. G. Bünzli, S. V. Eliseeva, in *Lanthanide Luminescence*, vol. 7 (Eds.: P. Hänninen, H. Härmä), Springer Verlag, Berlin, Heidelberg, **2011**, pp. 1–45.

[21] A. Beeby, I. M. Clarkson, R. S. Dickins, S. Faulkner, D. Parker, L. Royle, A. S. de Sousa, J. A. G. Williams, M. Woods, *J. Chem. Soc. Perkin Trans. 2* **1999**, 493–503.

[22] a) S. Aime, E. Gianolio, E. Terreno, G. B. Giovenzana, R. Pagliarin, M. Sisti, G. Palmisano, M. Botta, M. P. Lowe, D. Parker, *J. Biol. Inorg. Chem.* **2000**, *5*, 488–497; b) S. Dumas, V. Jacques, W. C. Sun, J. S. Troughton, J. T. Welch, J. M. Chasse, H. Schmitt-Willich, P. Caravan, *Invest. Radiol.* **2010**, *45*, 600–612.

[23] V. Jacques, S. Dumas, W. C. Sun, J. S. Troughton, M. T. Greenfield, P. Caravan, *Invest. Radiol.* **2010**, *45*, 613–624.

[24] a) G. Gonzalez, D. H. Powell, V. Tissieres, A. E. Merbach, *J. Phys. Chem.* **1994**, *98*, 53–59; b) K. Micskei, L. Helm, E. Brucher, A. E. Merbach, *Inorg. Chem.* **1993**, *32*, 3844–3850; c)

F. Botteman, G. M. Nicolle, L. Vander Elst, S. Laurent, A. E. Merbach, R. N. Muller, *Eur. J. Inorg. Chem.* **2002**, 2686–2693; d) S. Laurent, L. V. Houze, N. Guerit, R. N. Muller, *Helv. Chim. Acta* **2000**, *83*, 394–406; e) L. Vander Elst, F. Maton, S. Laurent, F. Seghi, F. Chapelle, R. N. Muller, *Magn. Reson. Med.* **1997**, *38*, 604–614.

[25] S. Laurent, L. Vander Elst, R. N. Muller, *Contrast Media Mol. Imaging* **2006**, *1*, 128–137.

[26] a) P. Lebduskova, P. Hermann, L. Helm, E. Toth, J. Kotek, K. Binnemans, J. Rudovsky, I. Lukes, A. E. Merbach, *Dalton Trans.* **2007**, 493–501; b) S. Aime, L. Calabi, C. Cavallotti, E. Gianolio, G. B. Giovenzana, P. Losi, A. Maiocchi, G. Palmisano, M. Sisti, *Inorg. Chem.* **2004**, *43*, 7588–7590; c) D. H. Powell, O. M. NiDhubhghaill, D. Pubanz, L. Helm, Y. S. Lebedev, W. Schlaepfer, A. E. Merbach, *J. Am. Chem. Soc.* **1996**, *118*, 9333–9346.

[27] a) N. Bloembergen, *J. Chem. Phys.* **1957**, *27*, 572–573; b) I. Solomon, *Phys. Rev.* **1955**, *99*, 559–565.

[28] J. H. Freed, *J. Chem. Phys.* **1978**, *68*, 4034–4037.

[29] L. Vander Elst, A. Sessoye, S. Laurent, R. N. Muller, *Helv. Chim. Acta* **2005**, *88*, 574–587.

[30] H. Onishi, K. Sekine, *Talanta* **1972**, *19*, 473–478.

[31] S. Huang, R. I. Endo, G. R. Nemerow, *J. Virol.* **1995**, *69*, 2257–2263.

Received: June 6, 2011
Published Online: July 15, 2011

